Detonation Propagation through Inhomogeneous Fuel-air Mixtures

Supraj Prakash and Venkat Raman
University of Michigan - Ann Arbor
Ann Arbor, MI, USA

1 Introduction

In practical rotating detonation engines (RDEs), non-premixed fuel and air injection is used to limit the back-propagation of high-pressure waves into the feed plenums. The incomplete fuel-air mixing in the near-injector region quenches the detonation process. However, this local stratification of fuel can persist leading to inefficient detonation propagation. Poorly-mixed gases have an effect similar to inert diluents on mixture detonability [1]. Following the passage of an azimuthally-processing detonation wave, partially-burnt gases within the base of the channel further impact detonability. Past numerical and experimental studies have investigated the impact of mixture concentration gradients on the detonation wave structure [2–5]. The mixture inhomogeneity results in a skewed detonation wave front, with irregular detonation cell structures and diminished wave propagation velocities. Gases with reduced detonability cause the reaction zone to decouple from the leading detonation wave, transitioning combustion to the deflagration mode, and reducing the detonation peak pressure [6, 7]. As concluded by Bykovskii et al. [8], the fuel-air mixing process is crucial in sustaining the continuous detonation regime for wave propagation.

Boulal et al. experimentally studied the effect of mixture composition gradients parallel to the direction of detonation propagation, stating that quenching is controlled by the composition gradient and the characteristic length [9]. Furthermore, transverse concentration gradients have been extensively studied by Boeck et al., where steep composition gradients do not quench detonation but rather diminish wave propagation velocities in comparison to those of homogeneous mixtures [5]. However, sharp concentration gradients result in single-headed, unstable detonation waves with "galloping" wave front behavior. Similarly, numerical simulations of transverse concentration gradients show that the instabilities promote flame acceleration and strong detonation-to-deflagration transition (DDT) in unobstructed channels [10], similar to the geometry studied here. Thus, overall detonation stability is affected due to the fuel concentration gradient, and rapid changes in the composition narrow the detonability envelope. Spatial inhomogeneity has been previously studied through one- and two-dimensional numerical simulations with single-step Arrhenius chemical kinetics by introducing a detonation wave to discrete reactive layers and squares, respectively [11]. With sufficiently inhomogeneous mixtures, where the spacing between successive reactive zones is greater than the reaction zone length, a "super-CJ" (Chapman Jouguet) wave behavior is observed, with propagation speeds 15 percent higher than the CJ speed of a homogeneous mixture [12]. Thus, discretely-placed fuel sources act as concentrated pockets of energy release and enforce a nonequilibrium state for the detonation wave.

Correspondence to: suprajp@umich.edu

In order to isolate the impact of mixture inhomogeneity on detonation propagation from the other complexities associated with a practical RDE, a canonical configuration is studied here. The study builds on past work through the use of detailed chemical kinetics in a three-dimensional domain. A confined channel filled with a stratified fuel-air mixture is processed using a detonation wave to determine the impact on wave propagation. The fuel stratification introduces composition gradients not purely aligned with the axial or transverse directions. To mimic the partial premixing and pre-mature combustion observed in full-scale RDEs, the fuel-air mixture is allowed to react for different total times (different levels of pre-burning) before the detonation wave is initiated. The next section details the simulation configuration and numerical details, with Sec. 3 providing the results and corresponding discussion.

2 Simulation Configuration and Computational Approach

To replicate the wave structure in a practical RDE geometry, a canonical channel geometry of length 14 cm, width 7.6 mm, and height 6.25 cm is modeled, as shown in Fig. 1. The height of the channel corresponds to the characteristic large length scale, L_{char}, within the domain. As an extension of past studies of Prakash et al. [13], the operating pressure of 0.5 atm with background air is used. The channel is confined with walls in the stream normal and spanwise direction, and the right boundary is set as an outflow. The inflow boundary condition is prescribed by a sampled right-running, well-developed, three-dimensional detonation wave. The grid resolution for the three-dimensional geometry is uniform with a core region in the stream normal and spanwise directions where cells are clustered near the wall to properly resolve the boundary layer. The clustered grid regions in the stream normal and spanwise directions extend up to 435 y^+ from the wall, where one y^+ is 0.6 μm. For all cases, the clustered grid region is characterized by Δy = Δz = 3.2-74.7 μm. Outside the core region, Δy = Δz = 75 μm, and Δx = 50 μm throughout the domain. The induction length ℓ, established as the length scale of interest, for stoichiometric hydrogen-air detonation at these operating conditions is analytically computed as 398 μm. Thus, approximately 8 and 5.3 points per induction length are used in the streamwise and stream normal/spanwise directions, respectively, for computational tractability.

A direct numerical simulation (DNS) approach is applied to study the detonation wave structure in canonical systems. The governing equations of fluid flow consist of mass, momentum, and energy conservation equations supplemented by species conservation equations that incorporate chemical reactions. The system of equations is closed using the ideal gas equation of state. The in-house compressible flow solver, UTCOMP, incorporates the Navier-Stokes equations in the compressible form and has been validated for a range of shock-containing flows [14–16]. The solver utilizes a structured grid configuration with a cell-centered, collocated variable arrangement. A 5$^{\text{th}}$ order weighted essentially non-oscillatory (WENO) scheme [17] is used for computing

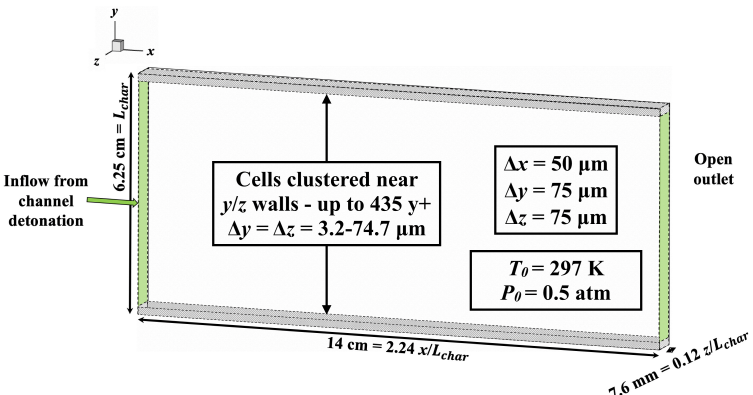

Figure 1: Three-dimensional channel domain with clustered cells near the wall.

the non-linear convective fluxes and the non-linear scalar terms are calculated using a quadratic upstream interpolation for convective kinematics (QUICK) scheme [18]. A 4$^{\text{th}}$ order central scheme is used to calculate the diffusive terms and a 4$^{\text{th}}$ order Runge-Kutta scheme is used for the temporal discretization.

The solver is parallelized using MPI-based domain decomposition and linear scalability has been demonstrated up to 65,000 cores for similar problems. The detailed chemical kinetics for hydrogen-oxygen combustion with a nitrogen diluter is provided by the 9-species 19-reaction chemical mechanism of Mueller et al. [19] using CHEMKIN-based subroutines [20]. The solver and chemical mechanism have been previously validated for hydrogen-air and hydrogen-oxygen detonation using one-, two- and three-dimensional canonical cases in Ref. [13].

Fuel-air stratification is introduced based on a method based used for turbulent mixing studies in homogeneous isotropic turbulence [21, 22]. Here, the stratification is assumed to be in fuel-air mixtures of a continuous range of equivalence ratios (fixed here as $\{0, 1.3\}$). An energy spectrum is assumed to provide the length scale distribution of these mixture patches. The spectrum uses an integral length scale as a parameter, which can be varied to create distributions of different length scales within the domain. This results in similar composition gradients across fuel patch boundaries among all the cases. With this process, fluctuations in the composition occur locally (across a length scale smaller than the domain) and the distribution is macroscopically "homogeneous" without the large-scale concentration gradients across the domain enforced in past numerical and experimental studies [5, 9]. Three cases - cases 1, 2, and 3 - with streamwise integral length scales of 0.581 mm (1.46ℓ), 0.894 mm (2.25ℓ), and 1.854 mm (4.66ℓ), respectively, are generated. To study the effect of pre-burning, the species mass fraction of this initial field (denoted by $Y(\boldsymbol{x}, 0)$) is allowed to proceed towards equilibrium as follows:

$$Y(\boldsymbol{x}, 0) = Y(\boldsymbol{x}, 0) + f\left(Y_{eq}(\boldsymbol{x}) - Y(\boldsymbol{x}, 0)\right), \tag{1}$$

where Y_{eq} denotes the equilibrium composition corresponding to the initial fuel mass fractions at a particular spatial location, and f is the fractional progress towards equilibrium. Four additional cases - cases 4, 5, 6, and 7 - are constructed with 25%, 50%, 75%, and 100% progression to the fully-burnt equilibrium condition, respectively. The initial fuel-air distributions are highlighted in Fig. 2.

Finally, an auxiliary calculation of detonation propagation in a channel of equivalent cross-section filled with a homogeneous stoichiometric hydrogen-air mixture is used to create a three-dimensional time-varying field. This is used as the inflow condition to introduce the detonation wave into the main simulation configuration. The well-developed, multi-headed detonation wave features triple points propagating along the front with a regular cell structure.

3 Results and Discussion on Fuel-air Stratification

The fully-developed detonation wave is introduced into the channel with the stratified fuel-air mixture in cases 1, 2, and 3. The detonation wave evolves very differently among the three cases, as visualized in Fig. 3. The stratification length scale directly affects the size of the vortical structures formed by the interaction of triple points and transverse wave stemming from the detonation wave front. The small eddy size of the finest stratification case results in a fairly planar wave front, with nodes of lower curvature along the front. The closer spacing of the triple points along the shock front corresponds to smaller detonation cell structures. While the cell width of case 3 closely resembles that of homogeneous hydrogen-air detonation,

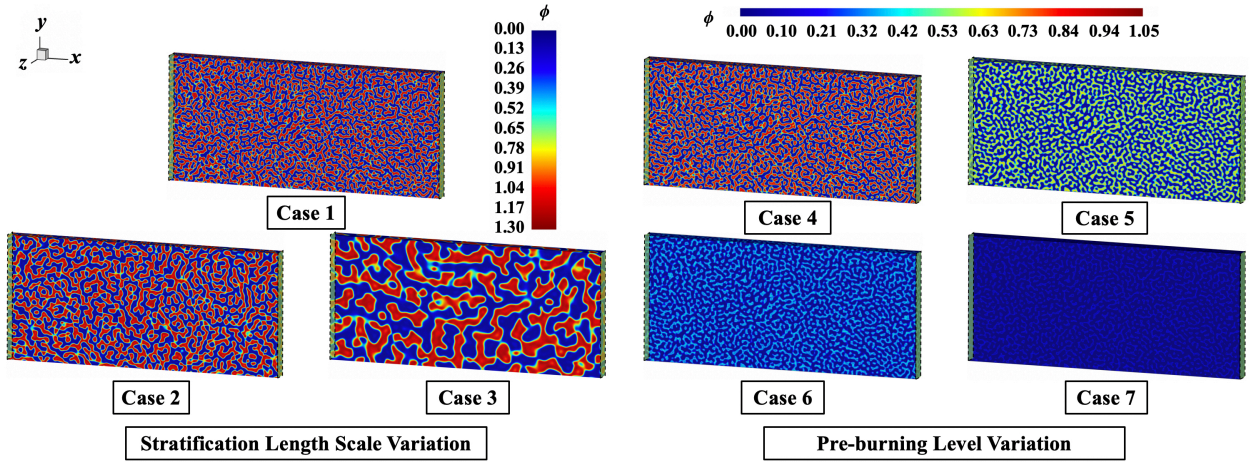

Figure 2: Fuel-air stratification within channel domain with varying stratification length scales (cases 1, 2, and 3) and levels of pre-burning (cases 4, 5, 6, and 7), displayed as equivalence ratio contour.

case 1 features a smaller cell size. Thus, by altering the stratification length scale, the detonation cell size is changed. With regard to RDE design, the stratification of the fuel and oxidizer within the annulus modifies the effective cell size, causing it to vary vastly from the homogeneous condition typically used for annulus sizing. The size of the vortical structures is directly proportional to the stratification length scale, and subsequently, the reaction zone (consisting of mixing regions and reflected pressure waves) broadens. As the wave passes through regions of background air, the leading shock front and trailing reaction zone separate as the detonation mode cannot be sustained. With the largest stratification length scale of case 3, this phenomena is more easily observed, with wave front velocities falling well below the CJ velocity in these regions. However, within regions of fuel, the wave propagation velocities increase above the theoretical CJ velocity for this mixture, similar to the super-CJ wave behavior observed by Mi et al. [11, 12]. Thus, the shock velocity spatial history is more homogeneous for case 1 than for case 3.

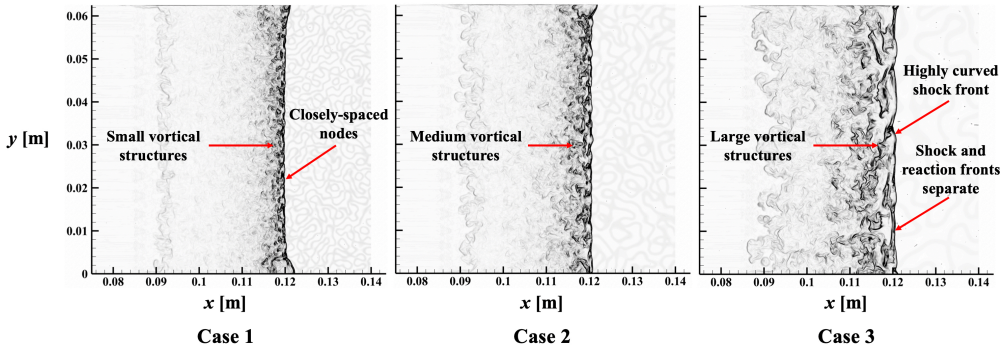

Figure 3: Numerical Schlieren images of the detonation wave as it nears the end of the channel domain, comparing the onset of turbulent mixing and eddy structures for cases 1, 2, and 3.

The large eddies are less efficient at mixing the residual and post-detonation gases within the reaction zone. This is evidenced by the detailed species behavior across the detonation wave, where cases 2 and 3 feature increasingly higher frequency and amplitude oscillations of species mass fraction within the reaction zone.

Similarly, the normalized standard deviation of flow properties and fuel mass fraction in the left plot of Fig. 4 highlight that the variance is proportional to stratification length scale. Behind the detonation wave front, case 1 features the lowest variability of pressure and temperature, although pressure disturbances (at the onset of the mixing region in the reaction zone at 500 μm behind the shock front) have a greater effect on the smaller stratification length scale cases. Interestingly, the fuel variability across the initial induction region is nearly identical for all three cases and the reaction progresses similarly. However, in the broader reaction zone, case 1 features the lowest normalized standard deviation of fuel mass fraction, suggesting a more homogeneous reaction zone with more complete consumption of fuel across the detonation wave. The right plot of Fig. 4 outlines two distinct modes of heat release: deflagration at low pressures and detonation at high pressures. There is increased heat release from low-pressure deflagration for case 1. On the other hand, heat release from detonation extends to higher pressures for the larger stratification length scale cases, suggesting stronger detonation. The increased intensity of heat release at lower pressures and leaner equivalence ratios for case 1 corresponds to increased deflagration in this configuration.

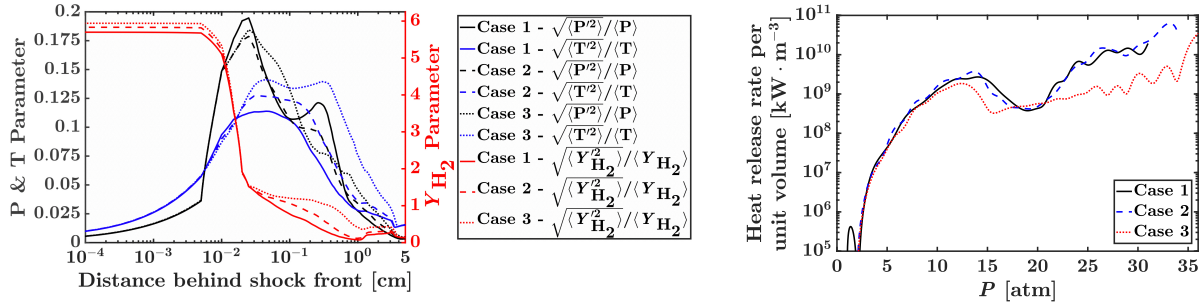

Figure 4: (Left) The streamwise-normal plane-averaged normalized standard deviation of pressure, temperature, and fuel mass fraction behind the detonation wave front for cases 1, 2, and 3. (Right) The average heat release per unit volume as a function of pressure in a region around the detonation wave for cases 1, 2, and 3.

4 Conclusions

The effect of fuel-oxidizer stratification length scale on the detonation wave structure has been studied through the direct numerical simulation of a confined channel detonation. A variation in the stratification length scale results in a competition between the detonation strength and overall combustion efficiency. The small eddy structures stemming from smaller stratification length scales are more efficient in mixing residual and post-detonation gases in the reaction zone. On the other hand, initial detonation wave strength is greater with larger stratification length scales, as the reaction proceeds to equilibrium closer to the shock front. In experiments of an RDE geometry, the detonation wave consists of an initial detonation wave followed by a broad region of deflagration. The small eddy structures of case 1 aid in this deflagration with higher combustion efficiency and a more homogeneous post-detonation mixture. Furthermore, the stratification level of the fuel-air mixture effectively changes the detonation cell size in comparison to that of homogeneous mixtures, affecting wave propagation behavior (single-headed as opposed to multi-headed) for a given channel width. Additional investigation of mixture inhomogeneity is required to further understand the dynamics of the detonation wave in practical RDEs. Future studies which induce a large-scale transverse or axial concentration gradient across the domain in combination with the small-scale fluctuations studied here may provide additional insight into practical RDE operation.

5 References

[1] V. N. Mikhalkin, "Thermodynamic calculation of detonation in poorly mixed gas mixtures," *Combustion, Explosion and Shock Waves*, vol. 32, pp. 57–60, Jan 1996.

[2] K. Ishii and M. Kojima, "Behavior of detonation propagation in mixtures with concentration gradients," *Shock Waves*, vol. 17, pp. 95–102, August 2007.

[3] D. Kessler, V. N Gamezo, and E. Oran, "Gas-phase detonation propagation in mixture composition gradients," *Philosophical transactions of the Royal Society. Series A, Mathematical, Physical, and Engineering Sciences*, vol. 370, pp. 567–96, 02 2012.

[4] D. Santavicca, R. Yetter, and S. Peluso, "Effect of mixture concentration inhomogeneity on detonation properties in pressure gain combustors." University Turbine Systems Research (UTSR) 2015 Kick-off Meeting (Presentation), October 2015.

[5] L. R. Boeck, F. M. Berger, J. Hasslberger, and T. Sattelmayer, "Detonation propagation in hydrogen–air mixtures with transverse concentration gradients," *Shock Waves*, vol. 26, pp. 181–192, Mar 2016.

[6] T. Sato, S. Voelkel, and V. Raman, "Detailed Chemical Kinetics based Simulation of Detonation Containing Flows." American Society of Mechanical Engineers (ASME) Turbo Expo, 2018.

[7] T. Sato and V. Raman, "Hydrocarbon fuel effects on non-premixed rotating detonation engine performance," AIAA SciTech Forum, American Institute of Aeronautics and Astronautics, Jan 2019.

[8] F. A. Bykovskii, S. A. Zhdan, and E. F. Vedernikov, "Continuous spin detonations," *Journal of Propulsion and Power*, vol. 22, pp. 1204–1216, Nov 2006.

[9] S. Boulal, P. Vidal, and R. Zitoun, "Experimental investigation of detonation quenching in non-uniform compositions," *Combustion and Flame*, vol. 172, pp. 222 – 233, 2016.

[10] R. K. Azadboni, A. Heidari, L. R. Boeck, and J. X. Wen, "The effect of concentration gradients on deflagration-to-detonation transition in a rectangular channel with and without obstructions a numerical study," *International Journal of Hydrogen Energy*, vol. 44, no. 13, pp. 7032 – 7040, 2019.

[11] X. Mi, A. J. Higgins, H. D. Ng, C. B. Kiyanda, and N. Nikiforakis, "Propagation of gaseous detonation waves in a spatially inhomogeneous reactive medium," *Phys. Rev. Fluids*, vol. 2, p. 053201, May 2017.

[12] X. Mi, E. V. Timofeev, and A. J. Higgins, "Effect of spatial discretization of energy on detonation wave propagation," *Journal of Fluid Mechanics*, vol. 817, p. 306338, 2017.

[13] S. Prakash, R. Fiévet, V. Raman, J. Burr, and K. H. Yu, "Analysis of the detonation wave structure in a linearized rotating detonation engine," 2018. Accepted to the AIAA Journal special issue on Continuous Detonation and its Applications.

[14] R. Fiévet and V. Raman, "Effect of vibrational nonequilibrium on isolator shock structure," 05 2018.

[15] R. Fiévet, H. Koo, and V. Raman, "Numerical simulation of a scramjet isolator with thermodynamic nonequilibrium," in *22nd AIAA Computational Fluid Dynamics Conference*, p. 3418, 2015.

[16] R. Fiévet, S. J. Voelkel, V. Raman, and P. L. Varghese, *Numerical investigation of vibrational relaxation coupling with turbulent mixing*. AIAA SciTech Forum, American Institute of Aeronautics and Astronautics, Jan 2017.

[17] G. Jiang and D. Peng, "Weighted eno schemes for hamilton–jacobi equations," *SIAM Journal on Scientific Computing*, vol. 21, no. 6, pp. 2126–2143, 2000.

[18] M. Herrmann, G. Blanquart, and V. Raman, "Flux corrected finite-volume scheme for preserving scalar boundedness in large-eddy simulations," in *43rd AIAA Aerospace Sciences Meeting and Exhibit - Meeting Papers*, pp. 4963–4972, 2005.

[19] M. A. Mueller, T. J. Kim, R. A. Yetter, and F. L. Dryer, "Flow reactor studies and kinetic modeling of the h2/o2 reaction," *International Journal of Chemical Kinetics*, vol. 31, no. 2, pp. 113–125, 1999.

[20] R. J. Kee, F. M. Rupley, and J. A. Miller, "Chemkin-ii: A fortran chemical kinetics package for the analysis of gas-phase chemical kinetics," tech. rep., United States, 1989.

[21] V. Eswaran and S. B. Pope, "Direct numerical simulations of the turbulent mixing of a passive scalar," *The Physics of Fluids*, vol. 31, no. 3, pp. 506–520, 1988.

[22] M. Hassanaly, V. Raman, H. Koo, and M. B. Colket, *Influence of Fuel Stratification on Turbulent Flame Propagation*. AIAA SciTech Forum, American Institute of Aeronautics and Astronautics, Jan 2015.